Pharmaceutical Research, Vol. 25, No. 8, August 2008 (© 2008)
DOI: 10.1007/s11095-008-9614-3

Research Paper

Enhancement in Anti-proliferative Effects of Paclitaxel in Aortic Smooth Muscle Cells upon Co-administration with Ceramide using Biodegradable Polymeric Nanoparticles

Dipti Deshpande,[1] Harikrishna Devalapally,[1] and Mansoor Amiji[1,2]

Received February 5, 2008; accepted April 28, 2008; published online May 15, 2008

Purpose. Using a combination of paclitaxel (PTX), and the apoptotic signaling molecule, C_6-ceramide (CER), the enhancement in anti-proliferative effect of human aortic smooth muscle cells (SMC) was examined by administering in polymeric nanoparticles.
Methods. PTX- and CER-loaded poly(ethylene oxide)-modified poly(epsilon caprolactone) (PEO-PCL) nanoparticles were formulated by solvent displacement and characterized. The uptake and intracellular localization of the nanoparticle in SMC was examined using Z-stack fluorescent confocal microscopy. Anti-proliferative and pro-apoptotic effects of SMC were determined upon administration of PTX and CER, either as single agent or in combination, in aqueous solution and in PEO-PCL nanoparticle formulations.
Results. High encapsulation efficiencies (i.e., >95%) of PTX and CER at 10% (*w*/*w*) loading were attained in the PEO-PCL nanoparticles of around 270 nm in diameter. Fluorescence confocal analysis showed that nanoparticle delivery did facilitate cellular uptake and internalization. Additionally, combination of PTX and CER delivery in PEO-PCL nanoparticles was significantly more effective in decreasing the proliferation of SMC, probably by enhancing the apoptotic response.
Conclusions. The results of this study show that combination of PTX and CER when administered in PEO-PCL nanoparticles can significantly augment the anti-proliferative effect in SMC. This strategy may potentially be useful in the treatment of coronary restenosis.

KEY WORDS: anti-proliferative effects; aortic smooth muscle cells; C_6-ceramide; coronary restenosis; paclitaxel.

INTRODUCTION

Removal of atherosclerotic plaque in the coronary artery is currently performed by invasive techniques, such as percutaneous transluminal coronary angioplasty (PTCA; commonly known as balloon angioplasty), atherectomy, and bare-metal stenting—together classified as percutaneous transluminal intervention (PTI) (1). All of these PTI procedures can lead to a complication called *restenosis* or intimal hyperplasia, which eventually leads to re-narrowing of the vessel and restriction of blood flow (2,3). Goldberg *et al.* (3,4) defined restenosis as a greater than 50% narrowing of the coronary artery as determined by a follow-up angiogram. Restenosis or decrease in the diameter of the coronary artery occurs in approximately 70% of the patients undergoing PTCA and atherectomy, and approximately in 15–50% of patients treated with implanted stents for the treatment of atherosclerosis (5–8). After stent placement, especially when the struts invade into the arterial wall leading to exposure of collagen, various molecular inflammatory signals are activated in the coronary artery (1,9). These inflammatory signals play a major role in restenosis and their levels correlates with the amount of injury at the site of stent deployment (10). With increase in the inflammatory process in the injured arterial wall, there is greater proliferation of vascular smooth muscle cells (SMC) in the lumen and narrowing of the artery (11).

For the treatment of restenosis, the Taxus® drug-eluting stent releases paclitaxel (PTX), embedded in a poly(styrene-*b*-isobutylene-*b*-styrene) (SIBS) triblock elastomeric polymer coating, over the lifetime of the patient (12). PTX is a potent anticancer chemotherapeutic agent, originally derived from the bark of the Pacific yew tree (*Taxus brevifolia*) (13), that is widely used in the treatment of solid tumors, particularly of the breast and ovaries (9). PTX exerts its cytotoxic effects by inducing tubulin polymerization resulting in unstable microtubules, which interferes with mitotic spindle function and ultimately arrests cells in the G2/M phase of mitosis (9). Tumor cells exposed to PTX treatment, as a result, then undergo programmed cell death or apoptosis (14). Although it is understood that cell cycle arrest results in activation of the apoptotic signaling cascade, recent studies suggest that PTX

[1] Department of Pharmaceutical Sciences, School of Pharmacy, Northeastern University, 110 Mugar Life Sciences Building, Boston, MA 02115, USA.
[2] To whom correspondence should be addressed. (e-mail: m.amiji@neu.edu)

therapy may also cause direct accumulation of endogenous ceramide, a lipid which functions as a cellular second messenger in apoptosis. Initial studies using PTX to prevent restenosis were performed by intravenous delivery. These studies showed that PTX used for prevention of SMC proliferation and intimal hyperplasia can be administered at much lower concentrations than those needed for cancer therapy (15–17).

In addition to PTX, membrane sphingolipids, such as ceramide (CER), that has been shown to enhance cellular apoptosis, has also been tested for the treatment of restenosis (18,19). Significant inhibition of restenosis was observed when CER coated angioplasty balloon was administered in a carotid artery stretch injury model established in New Zealand white rabbits (20). Accumulation of endogenous CER, produced by either hydrolysis or *de novo* synthesis, is known to result in response to several stimuli, such as growth factor deprivation, pro-inflammatory signals, exposure to increased temperature and radiation, and other stressors such as chemotherapeutics and related cytotoxic agents (21). Among such stimuli, PTX has been shown to elevate intracellular CER levels in a number of cell lines, including breast tumor cells (18).

In restenosis treatment, there is a critical need for alternative strategy to stent implantation. The major limitations of stent-based therapies include development of stent-related thrombosis, especially with drug-eluting stents as well as high rate of in-stent restenosis with the use of bare metal stents. In addition, optimum therapy for restenosis necessitates re-endothelialization of the coronary artery, which does not occur with any of the drug-eluting stents. As such, we hypothesized that biodegradable polymeric nanoparticles are well suited for intracellular drug delivery and the combination PTX and CER co-therapy will provide a synergistic anti-proliferative effect in the treatment of restenosis. Additionally, nanoparticle-based treatment of restenosis can be administered either local or by targeted systemic delivery, which is expected to lower systemic toxicity, while reaching specific cell types in sufficient concentrations for the necessary period of time, especially after intracellular uptake and localization (22). From the pioneering work of Labhasetwar and Levy (23,24), a number of other studies have examined the potential of nanoparticle-mediated delivery in restenosis. For instance, using fluorescently labeled polymeric nanoparticles, Westedt *et al.* (25) have shown a size dependency in arterial wall gene transfection administered in vivo with a SCIMED® REMEDY porous balloon catheter. Cells can incorporate particles varying from 50 to 300 nm in diameter based upon a variety of different internalization pathways including non-specific and receptor-mediated endocytosis (26–30). The bisphosphonate agent, alendronate, was encapsulated in a poly(D,L-lactide-*co*-glycolide) (PLGA) based nanoparticle system with an average size of 223 nm (31). When the formulation was administered intravenously in balloon injured rabbit artery model, there was significant reduction in neo-intimal growth. Beginning from the initial work of Suh *et al.* (32), PTX has also been incorporated in a number of nanoparticle formulations for restenosis therapy using various natural and synthetic polymers. The PTX concentration required for anti-proliferative effect and suppression of neo-intimal hyperplasia in restenosis in a stented rabbit model is significantly lower than typically used for cancer chemotherapy (15,16). The data indicated that after 28 days, neo-intimal SMC growth was inhibited with a single dose locally administered to the iliac bifurcation, while a second systemically administered dose was needed to see the effects prolonged out to 90 days. Doxorubicin, an anthracycline anticancer agent, and PTX were used in a tissue factor targeted lipid/perflorocarbon nanoemulsion to target vascular SMC proliferation *in vitro* using porcine SMC (33).

In a previous study, we have found that PTX and CER co-administration significantly enhances the cytotoxicity in a number of tumor cells, including multidrug resistant human ovarian and breast adenocarcinoma cells by lowering the apoptotic threshold (34). To examine the potential enhancement in anti-proliferative effect of PTX in SMC, in this study, we have encapsulated PTX and CER in poly(ethylene oxide)-modified poly(epsilon-caprolactone) (PEO-PCL) nanoparticles and have evaluated the anti-proliferative and pro-apoptotic effect using single and combination PTX and CER therapy in human aortic smooth muscle cells (SMC).

MATERIALS AND METHODS

Materials

PCL with a number average molecular weight of 14.8 kDa, as verified by gel-permeation chromatography, was purchased from Polysciences Inc. (Warrington, PA). National Formulary grade Pluronic® F-108 was kindly provided by the Performance Chemical Division of BASF Corporation (Parsinpanny, NJ). PTX was purchased from LC Laboratories (Woburn, MA). *N*-Hexanoyl-D-erythrosphingosine (C_6-CER) was purchased from Avanti Polar Lipids (Alabaster, AL). Human aortic SMC and the special culture media were purchased from Cell Applications, Inc., (San Diego, CA). Rhodamine-conjugated PTX was purchased from Natural Pharmaceuticals, Inc., (Beverley, MA). *N-a*-6-aminocaproyl-D-erythro-sphingosine (C_6-NBD-ceramide), propidium iodide, and YO-PRO®-1 were all purchased from Invitrogen (Carlsbad, CA). The MTT reagent, 3-(4,5-dimethylthiazol-2-yl)-2,5-diphenyltetrazolium bromide, and Dead-End™ Colorimetric Apoptosis Detection System (TUNEL assay) were purchased from Promega (Madison, WI). All the other chemicals and reagents were of analytical grade and were used as supplied. Deionized distilled water (NanoPure II, Dubuque, IA) was used for preparation of all aqueous solutions.

Preparation of PTX- and CER-containing PEO-PCL Nanoparticles

PEO-PCL nanoparticles were made by the solvent displacement method that has been used and optimized in our laboratory over the past several years (35–38). Briefly, 77 mg of PCL, purchased from Polysciences, Inc. (Warrington, PA), with a molecular weight of 12–14 kDa, as verified by gel filtration chromatography, was mixed with 13 mg of Pluronic® F-108 NF (BASF Corporation, Parsippany, NJ) in

3.0 ml of acetone (Fischer Scientific, Nutley, NJ). The polymer–acetone solution was then added drop-wise (~1.0 mL/min) into 25 mL of deionized distilled water under vigorous stirring at room temperature. The volume ratios of organic-to-aqueous phases, rate of addition, and the stirring speed have been optimized in order to produce nanoparticles with a mean diameter of between 150 and 300 nm. Once the organic phase contacted with the aqueous phase, the nanoparticles precipitated as was evident by formation of milky-white suspension. The stirring was continued for an additional 12 h to allow all of the organic solvent to evaporate and harden the nanoparticles. Following this period, the PEO-PCL nanoparticles were centrifuged for 10 min at 15,000 rpm using an ultracentrifuge, washed twice with deionized distilled water, and freeze-dried to obtain a free-flowing powder.

For incorporation of PTX, obtained from ICN (Aurora, IL), or *N*-hexanoyl-D-erythro-spingosine (C_6-CER), obtained from Avanti Polar Lipids (Alabaster, AL), in the PEO-PCL nanoparticles, 10 mg of each drug was dissolved in the acetone solution along with PCL and Pluronic® F-108. The drug-loaded nanoparticles were prepared exactly the same way as described above by adding the organic phase to the aqueous phase under vigorous stirring.

Characterization of PEO-PCL Nanoparticle Formulations

The formed PEO-PCL nanoparticles, with and without the encapsulated therapeutic agents, were characterized for particle size and size distribution, surface charge measurements, and surface morphological analysis.

Particle Size Analysis. The freeze-dried nanoparticles were re-suspended and diluted suitably in deionized distilled water and particle size was determined using the Brookhaven Instrument's (Holtsville, NY) 90-Plus particle size analyzer. This instrument uses light scattering principles to determine the effective hydrodynamic diameter of the nanoparticle in aqueous dispersion.

Surface Charge (Zeta Potential) Measurements. The surface charge on the nanoparticles is an important parameter to determine the stability of the aqueous dispersion and to assess whether the encapsulated therapeutic agent migrated to the surface or not upon drying of the nanoparticles. Surface charge (zeta potential) values of the blank and drug-loaded nanoparticles were measured using the Brookhaven Instrument's (Holtsville, NY) Zeta-PALS. The zeta potential was calculated using electrophoretic mobility of the nanoparticles in aqueous dispersion, made in deionized distilled water, using built-in software that uses the Smoluchowski–Helmholtz equation (39).

Scanning Electron Microscopy (SEM). SEM analysis provides surface morphological information and confirms the particle size values obtained using the light scattering method. SEM of the freeze-dried sample was performed using a Hitachi S-4800 (Pleasanton, CA) field emission scanning electron prepared exactly the same way as described above by adding the organic phase to the aqueous phase under vigorous stirring. The blank and drug-loaded samples were mounted on an aluminum sample mount and sputter-coated with gold–palladium to minimize surface charging. Sputter-coated samples were then observed with the electron microscopy and the digital images were processed with Adobe Photoshop® software.

Drug Encapsulation Efficiency. The loading capacity (i.e., micrograms of drug per milligram of nanoparticles) and efficiency (i.e., percent of the added drug that was loaded) of PTX and fluorescent-labeled CER in PEO-PCL nanoparticles was determined by dissolving a known amount in acetone and measuring the individual drug content either by UV absorbance (for PTX) or fluorescence spectroscopy (for CER). A UV standard curve of PTX and a fluorescence standard curve of NBD-C_6-CER in acetone were constructed and used to determine the amount of each agent in the nanoparticle formulation.

In Vitro Release of PTX and CER

The *in vitro* release studies of PTX and CER from the PEO-PCL nanoparticles were carried out in phosphate-buffered saline (PBS, pH 7.4) with 1% (*w*/*v*) Tween-80® at 37°C using a rotating platform. Tween-80®, a non-ionic surfactant of poly(ethylene glycol) and lauric acid (sorbitan monolaurate), was added to increase the solubility of the hydrophobic drugs in aqueous release medium and to prevent loss of drugs by binding to the container surfaces (40). For PTX, the solubility increases from 0.45 μg/ml in PBS to >10 μg/ml in PBS and 1% (*w*/*v*) Tween-80® at 37°C. At predetermined time points from 30 min to 24 h post-incubation, the samples were removed, centrifuged, and 5.0 mL the medium was collected. To maintain sink conditions, 5.0 mL of fresh PBS/Tween®-80 mixture was added back. The release medium was filtered through a 0.22 μm membrane filter.

For PTX release, a high performance liquid chromatography (HPLC) assay was used according to published procedure (41,42). For CER release studies, NBD-labeled C_6-CER was encapsulated in the PEO-PCL nanoparticles. The concentrations of CER released from the nanoparticles were determined by a fluorescence assay, where the excitation and emission wavelength were set at 485 and 530 nm, respectively. Using the standard curve of NBD-labeled CER in the release medium, cumulative amount and percent release were calculated.

Uptake and Distribution of PEO-PCL Nanoparticles in SMC

Cell Culture Conditions. Primary human aortic SMC, obtained from Cell Applications, Inc. (San Diego, CA), were cultured in special smooth muscle cell media also purchased from Cell Applications at 95% O_2 and 5% CO_2 incubation conditions at 37°C. For studying the nanoparticles uptake by fluorescent microscopy, SMC were grown on clean circular glass cover-slips placed in six-well plates.

Nanoparticle Uptake Studies. Fluorescently labeled PEO-PCL nanoparticles were prepared by incorporating 1% (*w*/*w*) rhodamine-labeled PTX into the organic phase along

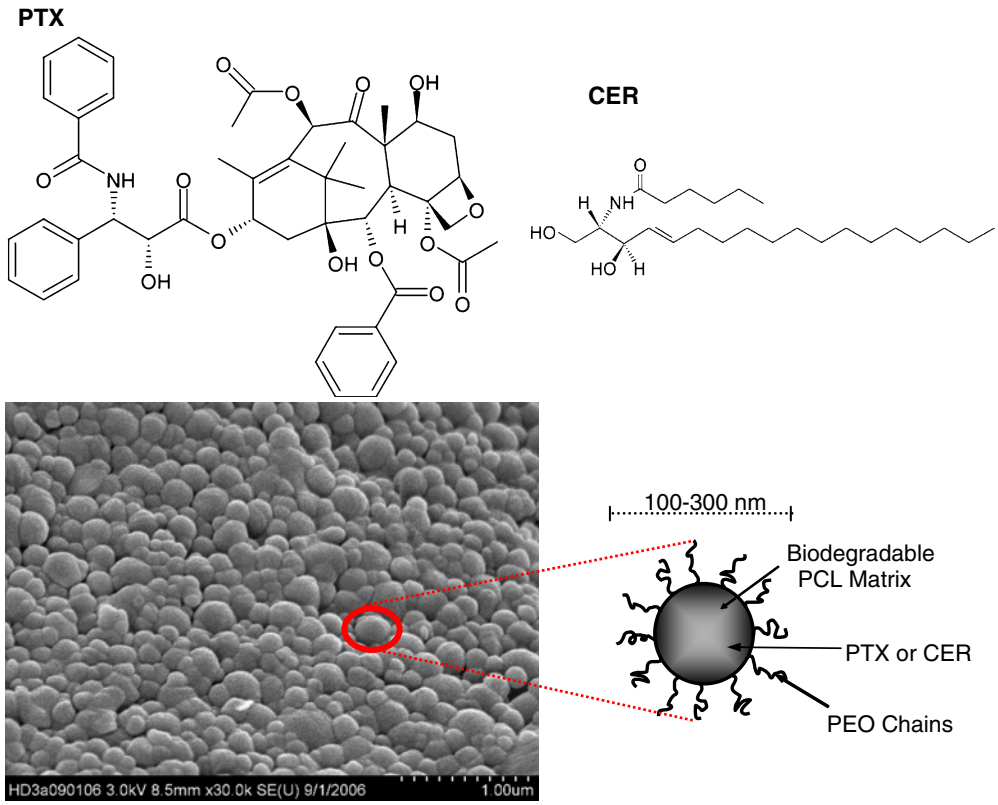

Fig. 1. The chemical structures of paclitaxel (*PTX*) and C_6-ceramide (*CER*) as well as the scanning electron micrograph of blank poly(ethylene oxide)-modified poly(epsilon-caprolactone) nanoparticles.

with the polymer while formulating the nanoparticles. Similarly, the fluorescently labeled PEO-PCL with CER was prepared by incorporating 1% (*w/v*) NBD-CER. The cover-slips were collected at periodic time intervals after washing the cells with sterile phosphate buffered saline (PBS, pH 7.4) and were mounted on glass slides using Fluoromount G®.

Z-stack Fluorescence Confocal Microscopy. The cellular uptake and internalization of the PTX-loaded and CER-loaded PEO-PCL nanoparticles in the SMC was determined by acquiring a time series of Z-stacks optical cross-sectional images in SMC. After an hour of drug administration, the cells were washed with phosphate buffered saline (PBS, pH 7.4) and the cover-slips were mounted over glass slides. The slides were then observed under Bio-Rad MRC 600 scanning confocal microscope (Bio-Rad, Hercules, CA) to obtain the Z-stacks of the cells. Each stack focused progressively at a depth of 2.0 μm within the cell and a series of three to ten stacks were obtained per cell. The stacks focused on the axial position of the fluorescently tagged nanoparticles enabling visualization of the location of these particles within the smooth muscle cells.

Anti-proliferative Effects of PTX and CER in SMC

The anti-proliferative effect of PTX and CER, when administered either in the aqueous solution or in PEO-PCL nanoparticles formulations, was examined in SMC cells. From previous studies of combination PTX and CER administration in tumor cells, we have selected the PTX concentration range from 0.10 to 100 nM and the CER concentration range from 10 nM to 30 μM. The cell viability was quantified by using the 3-(4,5-dimethylthiazol-2-yl)-2,5-diphenyltetrazolium bromide (MTT) assay. In this assay, the yellow-colored tetrazolium salts reagent is reduced to purple-colored formazan product by the action of mitochondrial dehydrogenase enzymes in living cells. For these studies, approximately 3,000 SMC suspended in specialized growth medium (Cell Applications, San Diego, CA) were seeded per well in a 96-well microplate and allowed to adhere for 24 h at 37°C and in 95% O_2/5% CO_2 atmosphere. The SMC in culture were treated with PTX and CER, either alone or in combination, in aqueous solution and in PEO-PCL nanoparticle formulation for 6 h. After this period, the cells were washed to remove

Table I. The Mean Particle Size and Zeta Potential of Paclitaxel and C_6-Ceramide Loaded Poly(Ethylene Oxide)-modified Poly(Epsilon-caprolactone) (PEO-PCL) Nanoparticles[a]

Nanoparticle formulation	Particle size (nM)	Zeta potential (mV)
Blank PEO-PCL nanoparticles	266.8±2.1	−17.81±1.10
Paclitaxel-loaded PEO-PCL nanoparticles	265.8±4.7	−22.18±1.13
C_6-Ceramide-loaded PEO-PCL nanoparticles	271±3.2	−19.36±1.27

[a] Mean ± SD (n=5)

Table II. Paclitaxel and C_6-Ceramide Loading Capacity and Efficiency in the Drug Loaded Nanoparticles

Nanoparticle system	Loading capacity (μg/mg)	Loading efficiency (%)
Paclitaxel-loaded PEO-PCL nanoparticles	95.0±1.86[a]	95.0±1.25
C_6 Ceramide-loaded PEO-PCL nanoparticles	96.0±2.43	96.2±1.47

[a] Mean ± SD (n=4)

any surface-bound drug or nanoparticles and the microplates were allowed to incubate for up to 6 days at 37°C. A cationic cytotoxic polymer, poly(ethyleneimine) (PEI) of 10,000 Da molecular weight, served as a positive control and untreated cells were used as negative control. After treatment, each well received 100 μL of MTT reagent (4 mg/mL) and the plates were incubated for 3 h. A cell lysis buffer at pH 4.7 consisting of 20% (*w*/*v*) of sodium lauryl sulfate, 50% (*w*/*v*) *N*,*N*-dimethylformamide was prepared. Following the incubation period, 100 μL the lysis buffer was added to each well and the system was further incubated for a period of 1 h. At the end of this incubation period, the formation of purple-colored formazan was monitored at 497 nm using a Bio-Tek microplate reader. The absorbance values were converted to percentage growth inhibition against negative control and reported as mean and standard deviation.

Pro-apoptotic Effects of PTX and CER in SMC

Quantitative Evaluation of Cellular Apoptosis. The Vybrant® Apoptosis assay kit #4 contained YO-PRO-1 and propium iodide, which was used to analyze the apoptotic activity by the flow cytometry. The smooth muscle cells were plated in six well plates at a cell density of 10×10^6 cells per well. Apoptosis was induced in the cells by treating the cells with of 2.0 and 20 nM of PTX and 200 nM and 1 μM of CER in aqueous solution and in PEO-PCL nanoparticles. A combined treatment of PTX loaded PEO-PCL nanoparticles with CER loaded PEO-PCL nanoparticles and PTX solution with CER solution was also administered. After 18 h of drug treatment, the cells were harvested using trypsin–EDTA and washed with cold PBS. The harvested cells were then suspended in 1 ml of PBS adjusting the cell density to 1×10^6 cells per milliliter. To 1.0 mL of the assay volume, 1.0 μL of the YO-PRO®-1 and 1 μL of the propium iodide solution were added for staining the cells. The controls used were smooth muscle cells treated with drug vehicles and then treated with YO-PRO®-1 and propium iodide individually as well as in combination. The cells were then incubated over ice for 30 min. After incubation, the cells were analyzed over the flow cytometer at an excitation of wavelength of 488 nm and two emission wavelengths; 530 nm for green fluorescence (YO-PRO®-1) and 610 nm for red fluorescence (propium iodide). A plot of fluorescence obtained with YO-PRO®-1 against the fluorescence obtained with propium iodide was used to calculate the percentage of live, necrotic, apoptotic and dead cells.

Qualitative Evaluations of Cellular Apoptosis. The DeadEnd® Colorimetric Apoptosis Detection System (Promega, Madison, WI) was used to visualize the apoptosis in SMC based on nuclear DNA fragmentation using the TUNEL procedure. The smooth muscle cells were plated over cover slips in clear six well plates at a cell density of 5×10^5 cells per well. Apoptosis was induced by treating the cells with the PTX loaded PEO-PCL nanoparticles (2 nM), CER loaded PEO-PCL nanoparticles (200 nM) and a combination therapy of the PTX and CER nanoparticles. Solutions containing 2.0 nM paclitaxel and 200 nM ceramide were also administered to induce apoptosis. After 12 h of drug treatment, the cover-slips with the treated cells were transferred onto glass slides and the cells were fixed using 10% buffered formalin at room temperature for 25 min. Following washing and permeabilization steps, 100 μL of recombinant terminal deoxynucleotidyl transferase (rTdT) mix (equilibration buffer + biotinylated nucleotide mix + rTdT enzyme) was added and the slides were incubated at 37°C for an hour. After washing, the cells were treated with 0.3% hydrogen peroxide in PBS for 5 min at room temperature, rinsed and washed with fresh PBS, treated with 100 μL of streptavidin-conjugated horse radish peroxidase in PBS and incubated for 30 min at room temperature. Finally, the cells were treated with the peroxidase substrate, diaminobenzene, for 10 min and the cover-slips with adherent cells were mounted on a slide using Flouromount G®. Samples were observed using a brightfield microscope and images were acquired and digitized.

Data Analysis

All of the results are reported as mean ± standard deviation and the differences between the control and test groups

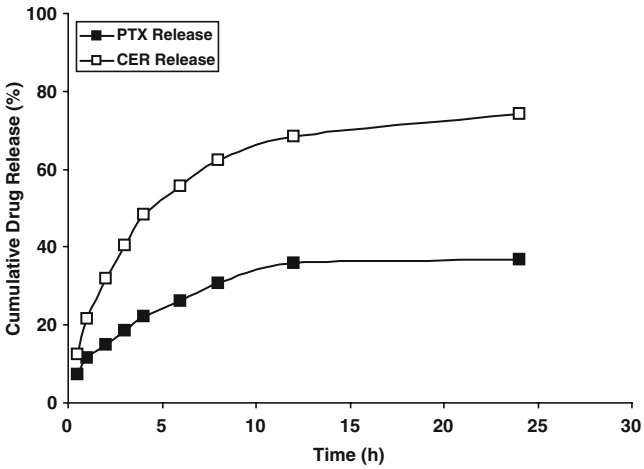

Fig. 2. *In vitro* release profiles of paclitaxel (*PTX*) and C_6-ceramide (*CER*) from poly(ethylene oxide)-modified poly(epsilon-caprolactone) nanoparticles in phosphate buffered saline (pH 7.4) at 37°C. Released PTX was quantified using a high performance liquid chromatography assay, while CER released was determined using NBD-labeled CER and fluorescence spectroscopy. The results show average and SD from three independent experiments.

were tested using Student's *t* test. Results were considered statistically significant between the control and test treatment at the level of $p<0.05$.

RESULTS AND DISCUSSION

Preparation and Characterization of PTX- and CER-loaded PEO-PCL Nanoparticles

Among various approved biodegradable and biocompatible polyesters, PCL possesses unique properties such as higher hydrophobicity and neutral biodegradation end products, which do not disturb the pH balance of the degradation medium (35,36). For surface modification of PCL nanoparticles, we have designed a system that utilizes the blend of PCL with Pluronic® F108 (poloxamer 407). Pluronics® are ABA triblock copolymers of poly(ethylene oxide)–poly(propylene oxide)–poly(ethylene oxide) (PEO–PPO–PEO), where the central hydrophobic PPO segment is expected to interact strongly with the hydrophobic PCL matrix, while the two hydrophilic PEO chains can extend into the aqueous environment. Pluronic® F-108 has 56 propylene oxide residues and 122 ethylene oxide residues and a molecular weight of 12,000 Da. The assembly of Pluronic® F-108 with PCL leaves the hydrophilic PEO side-arms in a mobile state as they extend outwards from the particle surface and provide stability to the nanoparticle in aqueous suspension by a repulsion effect through a steric mechanism of stabilization involving both enthalpic and entropic contributions.

Fig. 1 shows the SEM image of blank PEO-PCL nanoparticles. The formulations containing PTX and CER also were similar to the blank nanoparticles under SEM evaluations. The nanoparticles had a spherical shape with smooth surface. The results of particle size, presented in Table I, confirm the SEM data to show an average hydrodynamic diameter of the blank PEO-PCL nanoparticles to be approximately 270 nm. Inclusion of PTX and CER did not significantly increase the particle size. Additionally, the surface charge of blank and both drug loaded nanoparticles was around −16 to −22 mV, and it was observed that the drug loaded nanoparticles had a surface charge value similar to those of the blank nanoparticles. This is indicative of the fact that both PTX and CER were encapsulated in the nanoparticle matrix and did not adsorb or migrate to the surface.

PTX- and CER-loaded PEO-PCL nanoparticles were dissolved in acetone and the loading capacity and efficiency was determined. As shown in Table II, both PTX and CER were efficiently encapsulated in PEO-PCL nanoparticles. The average loading capacities of PTX and CER were 95.0 and 96.2 μg/mg of nanoparticles, respectively. These loading capacity values correspond to 95.0% and 96.2% loading efficiencies of PTX and CER, respectively.

The *in vitro* release studies of PTX and CER from PEO-PCL nanoparticles was evaluated over a period of 24 h at 37°C. The release profile in Fig. 2 shows that PTX was released slowly from the hydrophobic polymer matrix as compared to CER. After 6 h of incubation, an average of 22% PTX release occurred, while more than 60% of the encapsulated CER was released in the same period. In addition, at 24 h, a maximum of 37% of PTX and 74% CER were released from the PEO-PCL nanoparticles in the simulated environments.

Evidence of Nanoparticle Internalization in SMC by Fluorescence Microscopy

The results in Fig. 3 represent the cellular internalization of the PTX and CER nanoparticles in SMC. Z-stack analysis was performed using scanning confocal microscopy and the images of the various optical slices are shown. Each optical slice was approximately 2 μm in thickness along the *Z*-axis as shown in Fig. 3a. PTX and CER cellular internalization in SMC cells using PEO-PCL nanoparticles Fig. 3b [(a) through (h)] and Fig. 3c [(a) through (h)] shows that the nanoparticle did facilitate internalization of the two fluorescent compounds. There was increasingly brighter fluorescence along the Z-stack from (a) through (h). If the nanoparticles were adsorbed to the surface of the cell, the fluorescence intensities in both cases would have decreased along the *Z*-axis.

Anti-proliferative Effects of PTX and CER in SMC

Initial studies to examine the effects of PTX and CER effects in SMC were performed with single agents administered either in aqueous solution or in PEO-PCL nanoparticles. Blank PEO-PCL nanoparticles without any drugs did not have any cytotoxicity at the doses used for administration of PTX and CER in this study. As shown from the results in Fig. 4, administration of PTX and CER in nanoparticle formulations enhanced the anti-proliferative effects in SMC as determined by MTT (formazan) assay. The cell viability versus PTX concentration curve (Fig. 4a) was slightly right-shifted with administration in PEO-PCL nanoparticles. The PTX IC_{50} (i.e., drug concentration that causes 50% decrease in cell viability) was determined to be 3.74 nM for aqueous solution and 1.80 nM for the PEO-PCL nanoparticles. Other groups have reported similar IC_{50} values (~2.0 to 4.0 nM) for PTX in SMC when administered in solution (17).

There was significantly higher right-shift in the cell viability versus concentration profile of CER when administered in PEO-PCL nanoparticles as compared to aqueous solution formulation (Fig. 4b). Although C_6-CER is cell-permeable, encapsulation in PEO-PCL nanoparticles results in greater intracellular availability relative to aqueous solution, especially at lower concentrations, when examined in SKOV3 human ovarian adenocarcinoma cells (34). Additionally, CER is susceptible to enzymatic hydrolysis in cell culture environment and *in vivo*. The CER IC_{50} values were found to be 4.4 μM in solution formulation and only 0.16 μM when administered in PEO-PCL nanoparticles. More than 27-fold decrease in IC_{50} of CER with the PEO-PCL nanoparticles was due to increased intracellular bioavailability of CER when administered in the nanoparticle formulation.

In order to examine the synergistic effect of combination of PTX and CER, the two drugs were administered at concentrations below the IC_{50} value for the PEO-PCL nanoparticles (i.e., PTX was administered at 1 and 2 nM

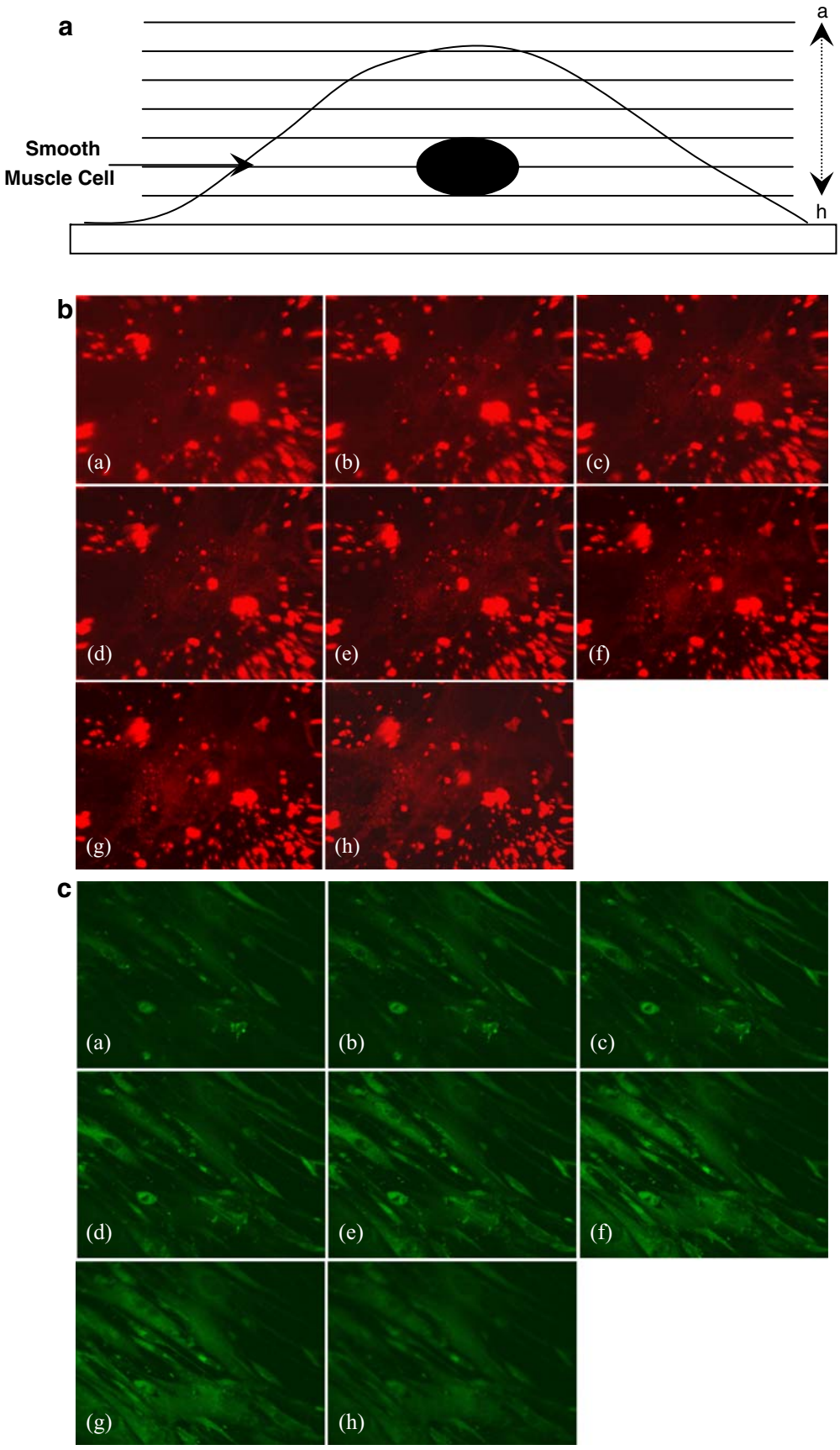
a
Smooth
Muscle Cell
a
h
b
(a)
(b)
(c)
(d)
(e)
(f)
(g)
(h)
c
(a)
(b)
(c)
(d)
(e)
(f)
(g)
(h)

◀ **Fig. 3.** Z-stack fluorescence confocal microscopy analysis of rhodamine-labeled paclitaxel and NBD-labeled C_6-ceramide administered in poly(ethylene oxide)-modified poly(epsilon-caprolactone) (PEO-PCL) nanoparticles in human aortic smooth muscle cells. Schematic illustration of Z-stack analysis with approximately 2 μm optical cross-sectional image acquisition (**a**), cellular internalization of rhodamine-labeled paclitaxel encapsulated in PEO-PCL nanoparticle (**b**), and cellular internalization of NBD-ceramide encapsulated in PEO-PCL nanoparticle (**c**). All of the images were acquired at ×20 magnification.

concentrations and CER was administered at 100 and 200 nM concentrations). Although there was some discrepancy in the results when PTX and CER were administered as single agent, the results in Fig. 4c clearly show that co-administration of PTX and CER was significantly more effective in the anti-proliferative activity in SMC as compared to PTX or CER as single agents. In addition, administration of PTX and CER in PEO-PCL nanoparticles was significantly more effective that aqueous solution formulations. For instance, the average percent cell viability was 62.4% and 27.9% when PTX and CER were administered at 1 and 100 nM concentrations in aqueous solution and PEO-PCL nanoparticles, respectively. When the drug doses were increased to 2 nM PTX and 200 nM CER, the average cell viability was 25.5% in aqueous solution and only 5.7% in PEO-PCL nanoparticles. These results clearly show that co-administration of PTX and CER, especially in PEO-PCL nanoparticles, results in significant anti-proliferative effects in SMC.

Apoptotic Activity of PTX and CER in SMC Cells

Since CER is known to be an apoptotic second messenger and exogenous CER administration has already proven efficacy in enhancing PTX activity in a number of tumor cells and *in vivo* (34,43), it was important to examine the apoptotic activity of combination PTX and CER administration in SMC. At the doses selected for administration of PTX and CER, the cellular apoptotic activity from blank PEO-PCL nanoparticle treatment was similar to the untreated cells. The results in Fig. 5 shows quantitative apoptotic activity by performing the Vybrant® Apoptosis assay using flow cytometry. In this assay, the YO-PRO®-1 (green, apoptotic cell permeant) dye and propium iodide (red, apoptotic cell impermeant) are used to label and differentiate between the live cells, those undergoing apoptosis, and those that are dead. Apoptosis in SMC was induced by treating the cells for 18 h with 2.0 and 20 nM PTX and 200 nM and 1.0 μm CER, either alone or in combination, administered in aqueous solution or in PEO-PCL nanoparticles formulations. The rationale for selection of higher concentrations of PTX and CER (i.e., 200 nM and 1.0 μM, respectively) was to evaluate if further apoptosis was evident since these studies were carried out for only 18 h as compared to 6 days for the anti-proliferation studies.

The scatter plots show that there was enhancement in cellular apoptosis when PTX and CER were administered in PEO-PCL nanoparticles as compared to aqueous solution formulation. Administration of CER at 200 nM and 1.0 μM in PEO-PCL nanoparticles also showed around 54% apoptosis. In addition, when PTX and CER co-therapy was administered with PEO-PCL nanoparticles, there was an increase in apoptosis at lower doses (i.e., 56.3% apoptosis with 2 nM PTX and 200 nM CER). However, the enhancement in apoptosis was not evident at higher doses (only 39.0% with 20 nM PTX and 1.0 μM CER). It is not entirely clear why the cellular apoptotic activity decreases with increase in the PTX

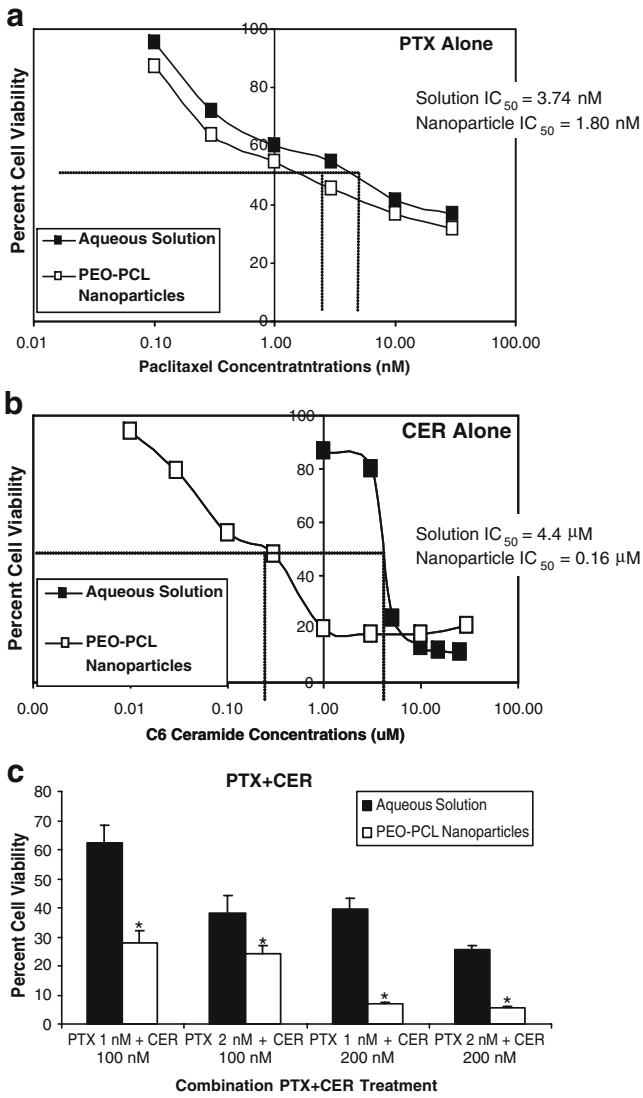

Fig. 4. Anti-proliferative effect of paclitaxel (*PTX*) and C_6-ceramide (*CER*) when administered in human aortic smooth muscle cells (SMC) in aqueous solution and in poly(ethylene oxide)-modified poly (epsilon-caprolactone) (*PEO-PCL*) nanoparticle formulations. Percent cell viability as a function of PTX concentrations and the determination of IC_{50} values of PTX in SMC (**a**), percent cell viability as a function of CER concentrations and the determination of IC_{50} values of CER in SMC (**b**), and co-administration of PTX and CER in SMC (**c**). The cell viability analysis, using MTT (formazan) assay, was performed after 6 days of treatment. The results show average and SD from three independent experiments (*asterisk*, $p<0.05$ relative to aqueous solution formulation).

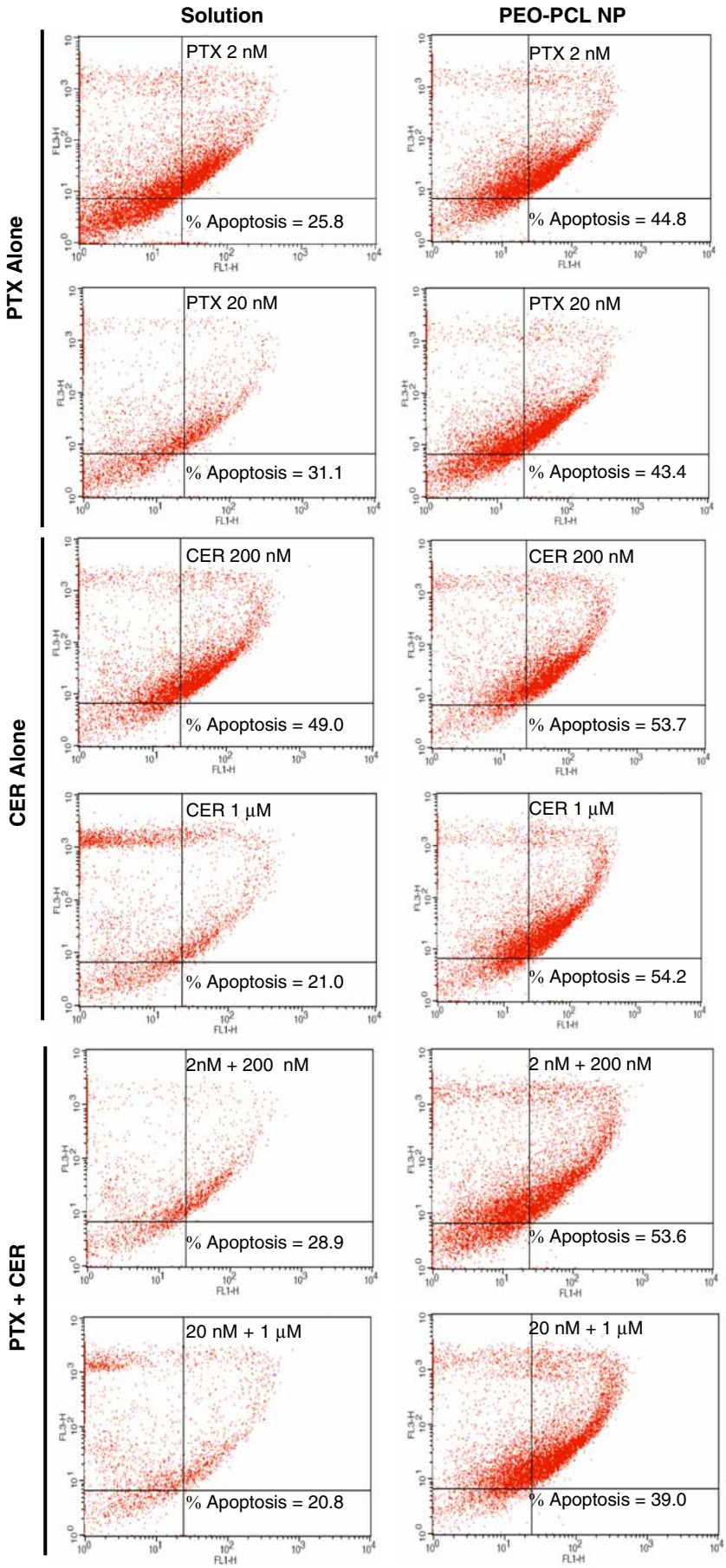
Solution
PEO-PCL NP
PTX Alone
CER Alone
PTX + CER
PTX 2 nM
% Apoptosis = 25.8
PTX 2 nM
% Apoptosis = 44.8
PTX 20 nM
% Apoptosis = 31.1
PTX 20 nM
% Apoptosis = 43.4
CER 200 nM
% Apoptosis = 49.0
CER 200 nM
% Apoptosis = 53.7
CER 1 µM
% Apoptosis = 21.0
CER 1 µM
% Apoptosis = 54.2
2nM + 200 nM
% Apoptosis = 28.9
2 nM + 200 nM
% Apoptosis = 53.6
20 nM + 1 µM
% Apoptosis = 20.8
20 nM + 1 µM
% Apoptosis = 39.0
FL1-H
FL3-H

◀ **Fig. 5.** Quantitative apoptotic activity of paclitaxel and C_6-ceramide when administered in human aortic smooth muscle cells in aqueous solution and in poly(ethylene oxide)-modified poly(epsilon-caprolactone) (*PEO-PCL*) nanoparticle formulations. Flow cytometric analysis using YO-PRO® and propidium iodide assay was performed with PTX in solution and in PEO-PCL nanoparticles at 2 and 20 nM doses, CER in solution and in PEO-PCL nanoparticles at 200 nM and 1.0 μm doses, and the combination of PTX and CER administered at 2 and 200 or 20 nM and 1.0 μm doses of PTX and CER, respectively. Flow cytometric analyses were performed after 18 h of treatment.

and CER doses using PEO-PCL nanoparticles. This may be either due to lack of nanoparticle internalization as a result of saturation of the non-specific endocytotic uptake or decreased intracellular availability of the drugs (34,36). However, in each case, the PEO-PCL nanoparticle-mediated delivery was significantly more effective in inducing apoptosis relative to aqueous solution indicating enhancement in drug internalization (especially CER) in SMC.

Additional qualitative evidence of apoptotic activity upon administration 2 nM PTX and 200 nM CER administrations in aqueous solution and in PEO-PCL nanoparticles was obtained using TUNEL assay. TUNEL assay examines apoptosis as a result of DNA fragmentation occurring in the SMC due to PTX and CER single and combination therapy. In the DeadEnd™ Colorimetric TUNEL assay system, upon DNA fragmentation, the apoptotic nuclei are stained brown by a three-step mechanism that involves incorporation of biotinylated nucleotides at 3′-OH DNA end, binding of horseradish peroxidase-labeled streptavidin to the incorporated nucleotides, and finally the detection of the nucleotides with the help of peroxidase substrate, diaminobenzidine, which results in the formation of the dark brown stains.

As observed in Fig. 6, the SMCs treated with blank nanoparticles and blank solution (DMSO) show no brown nuclei. In addition, the cells treated with PTX and CER in aqueous solution also did not show significant apoptotic activity. However, when the cells were treated with PTX- and CER-loaded nanoparticles, there was the characteristics dark brown staining of the nuclei that is representative of apoptotic cells. Combination PTX and CER therapy, when administered in PEO-PCL nanoparticles resulted in the highest degree of apoptosis and led to the most pronounced dark brown staining. The enhancement in staining is probably due to a greater degree of apoptotic activity with combination nanoparticle-delivered therapy.

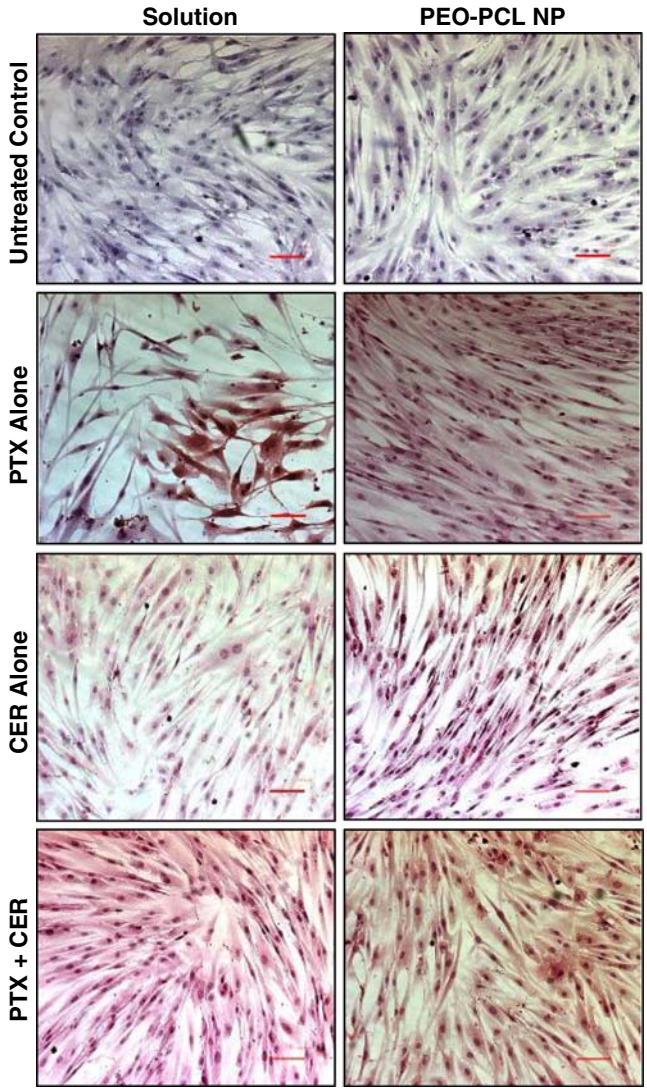

Fig. 6. Qualitative analysis of cellular apoptosis in human aortic smooth muscle cells (SMC), using TUNEL assay, upon treatment with paclitaxel (*PTX*) and C_6-ceramide (*CER*), either alone or in combination, in aqueous solution and in poly(ethylene oxide)-modified poly(epsilon-caprolactone) (*PEO-PCL*) nanoparticle formulations. The SMC were treated with 2 nM PTX and 200 nM of CER, either alone or in combination, administered in solution or in PEO-PCL nanoparticles for 12 h. Original magnification was ×10.

CONCLUSIONS

Coronary restenosis is associated with an increase in the proliferation of aortic SMC due to disruption of the endothelial cell layer in the lumen after balloon angioplasty and other treatment modalities for atherosclerosis. PTX has been used successfully to minimize SMC proliferation with drug-eluting stents. In order to enhance the anti-proliferative effects of PTX, in this study, we have examined co-administration with CER in PEO-PCL nanoparticles. The results show that PEO-PCL nanoparticles can efficiently encapsulate both PTX and CER and afford intracellular availability in SMC. CER alone, when administered in PEO-PCL nanoparticles, was significantly effective in anti-proliferative effect as well as cellular apoptosis. The combination PTX and CER administration, especially in PEO-PCL nanoparticle formulations, did enhance the anti-proliferative effects. There results are highly encouraging and serve to suggest that PEO-PCL nanoparticle delivery of PTX and CER combination could potentially have significant benefit in the treatment of coronary restenosis.

REFERENCES

1. G. Dangas, and F. Kuepper. Cardiology patient page. Restenosis: repeat narrowing of a coronary artery: prevention and treatment. *Circulation*. **105**:2586–2587 (2002).
2. T. Uwatoku, H. Shimokawa, K. Abe, Y. Matsumoto, T. Hattori, K. Oi, T. Matsuda, K. Kataoka, and A. Takeshita. Application of nanoparticle technology for the prevention of restenosis after balloon injury in rats. *Circ. Res.* **92**:e62–e69 (2003).
3. K. Ganesan, and B. Balram. Prevention of restenosis after coronary angioplasty [Prevention]. *Curr. Opin. Cardiol.* **19**:500–509 (2004).
4. S. L. Goldberg, A. Loussararian, J. De Gregorio, C. Di Mario, R. Albiero, and A. Colombo. Predictors of diffuse and aggressive intra-stent restenosis. *J. Am. Coll. Cardiol.* **37**:1019–1025 (2001).
5. M. Bennett. In-stent stenosis: pathology and implications for the development of drug eluting stents. *Heart (BMJ)*. **89**:218–224 (2003).
6. F. Airoldi, C. Di Mario, G. Stankovic, C. Briguori, E. Bramucci, B. Reimers, D. Ardissino, E. Aurier, D. Tavano, and A. Colombo. Effectiveness of treatment of in-stent restenosis with an 8-French compatible atherectomy catheter. *Am. J. Cardiol.* **92**:725–728 (2003).
7. J. Sharma, R. Kashyap, and A. Sharma. Restenosis following percutaneous transluminal coronary angioplasty among aircrew during intermediate and long term follow up. *Ind. J. Aerospace Med.* **47**:17–22 (2003).
8. H. J. Rapold, P. R. David, P. Guiteras Val, A. L. Mata, P. A. Crean, and M. G. Bourassa. Restenosis and its determinants in first and repeat coronary angioplasty. *Eur. Heart J.* **8**:575–586 (1987).
9. M. A. Costa, and D. I. Simon. Molecular basis of restenosis and drug-eluting stents. *Circulation*. **111**:2257–2273 (2005).
10. F. G. Welt, and C. Rogers. Inflammation and restenosis in the stent era. *Arterioscler. Thromb. Vasc. Biol.* **22**:1769–1776 (2002).
11. C. P. Regan, P. J. Adam, C. S. Madsen, and G. K. Owens. Molecular mechanisms of decreased smooth muscle differentiation marker expression after vascular injury. *J. Clin. Invest.* **106**:1139–1147 (2000).
12. S. V. Ranade, K. M. Miller, R. E. Richard, A. K. Chan, M. J. Allen, and M. N. Helmus. Physical characterization of controlled release of paclitaxel from the TAXUS Express2 drug-eluting stent. *J. Biomed. Mater. Res. A*. **71**:625–634 (2004).
13. J. D. Adams, K. P. Flora, B. R. Goldspiel, J. W. Wilson, S. G. Arbuck, and R. Finley. Taxol: a history of pharmaceutical development and current pharmaceutical concerns. *J. Natl. Cancer Inst. Monogr.* **15**:141–147 (1993).
14. M. Pennati, A. J. Campbell, M. Curto, M. Binda, Y. Cheng, L. Z. Wang, N. Curtin, B. T. Golding, R. J. Griffin, I. R. Hardcastle, A. Henderson, N. Zaffaroni, and D. R. Newell. Potentiation of paclitaxel-induced apoptosis by the novel cyclin-dependent kinase inhibitor NU6140: a possible role for survivin down-regulation. *Mol. Cancer. Ther.* **4**:1328–1337 (2005).
15. S. J. Sollott, L. Cheng, R. R. Pauly, G. M. Jenkins, R. E. Monticone, M. Kuzuya, J. P. Froehlich, M. T. Crow, E. G. Lakatta, E. K. Rowinsky, *et al*. Taxol inhibits neointimal smooth muscle cell accumulation after angioplasty in the rat. *J. Clin. Invest.* **95**:1869–1876 (1995).
16. C. Herdeg, M. Oberhoff, A. Baumbach, A. Blattner, D. I. Axel, S. Schroder, H. Heinle, and K. R. Karsch. Local paclitaxel delivery for the prevention of restenosis: biological effects and efficacy in vivo. *J. Am. Coll. Cardiol.* **35**:1969–1976 (2000).
17. D. I. Axel, W. Kunert, C. Goggelmann, M. Oberhoff, C. Herdeg, A. Kuttner, D. H. Wild, B. R. Brehm, R. Riessen, G. Koveker, and K. R. Karsch. Paclitaxel inhibits arterial smooth muscle cell proliferation and migration in vitro and in vivo using local drug delivery. *Circulation*. **96**:636–645 (1997).
18. R. Kolesnick. The therapeutic potential of modulating the ceramide/sphingomyelin pathway. *J. Clin. Invest.* **110**:3–8 (2002).
19. F. D. Kolodgie, A. Farb, and R. Virmani. Local delivery of ceramide for restenosis: is there a future for lipid therapy? *Circ. Res.* **87**:264–267 (2000).
20. R. Charles, L. Sandirasegarane, J. Yun, N. Bourbon, R. Wilson, R. P. Rothstein, S. W. Levison, and M. Kester. Ceramide-coated balloon catheters limit neointimal hyperplasia after stretch injury in carotid arteries. *Circ. Res.* **87**:282–288 (2000).
21. C. E. Chalfant, B. Ogretmen, S. Galadari, B. J. Kroesen, B. J. Pettus, and Y. A. Hannun. FAS activation induces dephosphorylation of SR proteins; dependence on the de novo generation of ceramide and activation of protein phosphatase 1. *J. Biol. Chem.* **276**:44848–44855 (2001).
22. L. Brito, and M. Amiji. Nanoparticulate carriers for the treatment of coronary restenosis. *Int. J. Nanomed.* **2**:143–161 (2007).
23. V. Labhasetwar, C. Song, W. Humphrey, R. Shebuski, and R. J. Levy. Arterial uptake of biodegradable nanoparticles: effect of surface modifications. *J. Pharm. Sci*. **87**:1229–1234 (1998).
24. C. Song, V. Labhasetwar, X. Cui, T. Underwood, and R. J. Levy. Arterial uptake of biodegradable nanoparticles for intravascular local drug delivery: results with an acute dog model. *J. Control Release*. **54**:201–211 (1998).
25. U. Westedt, L. Barbu-Tudoran, A. K. Schaper, M. Kalinowski, H. Alfke, and T. Kissel. Deposition of nanoparticles in the arterial vessel by porous balloon catheters: localization by confocal laser scanning microscopy and transmission electron microscopy. *AAPS Pharm. Sci.* **4**:E41 (2002).
26. S. Mukherjee, R. N. Ghosh, and F. R. Maxfield. Endocytosis. *Physiol. Rev.* **77**:759–803 (1997).
27. J. Gruenberg. The endocytic pathway: a mosaic of domains. *Nat. Rev. Mol. Cell. Biol.* **2**:721–730 (2001).
28. L. Pelkmans, and A. Helenius. Endocytosis via caveolae. *Traffic*. **3**:311–320 (2002).
29. S. B. Sieczkarskiand, and G. R. Whittaker. Dissecting virus entry via endocytosis. *J. Gen. Virol.* **83**:1535–1545 (2002).
30. S. A. Mousavi, L. Malerod, T. Berg, and R. Kjeken. Clathrin-dependent endocytosis. *Biochem. J.* **377**:1–16 (2004).
31. H. Cohen-Sacks, Y. Najajreh, V. Tchaikovski, G. Gao, V. Elazer, R. Dahan, I. Gati, M. Kanaan, J. Waltenberger, and G. Golomb. Novel PDGFbetaR antisense encapsulated in polymeric nanospheres for the treatment of restenosis. *Gene. Ther.* **9**:1607–1616 (2002).
32. H. Suh, B. Jeong, R. Rathi, and S. W. Kim. Regulation of smooth muscle cell proliferation using paclitaxel-loaded poly(ethylene oxide)–poly(lactide/glycolide) nanospheres. *J. Biomed. Mater. Res.* **42**:331–338 (1998).
33. G. M. Lanza, X. Yu, P. M. Winter, D. R. Abendschein, K. K. Karukstis, M. J. Scott, L. K. Chinen, R. W. Fuhrhop, D. E. Scherrer, and S. A. Wickline. Targeted antiproliferative drug delivery to vascular smooth muscle cells with a magnetic resonance imaging nanoparticle contrast agent: implications for rational therapy of restenosis. *Circulation*. **106**:2842–2847 (2002).
34. L. E. van Vlerken, Z. Duan, M. V. Seiden, and M. M. Amiji. Modulation of intracellular ceramide using polymeric nanoparticles to overcome multidrug resistance in cancer. *Cancer Res.* **67**:4843–4850 (2007).
35. J. S. Chawla, and M. M. Amiji. Biodegradable poly(epsilon-caprolactone) nanoparticles for tumor-targeted delivery of tamoxifen. *Int. J. Pharm.* **249**:127–138 (2002).
36. J. S. Chawla, and M. M. Amiji. Cellular uptake and concentrations of tamoxifen upon administration in poly(epsilon-caprolactone) nanoparticles. *AAPS Pharm. Sci.* **5**:E3 (2003).
37. L. K. Shah, and M. M. Amiji. Intracellular delivery of saquinavir in biodegradable polymeric nanoparticles for HIV/AIDS. *Pharm. Res.* **23**:2638–2645 (2006).
38. D. Shenoy, S. Little, R. Langer, and M. Amiji. Poly(ethylene oxide)-modified poly(beta-amino ester) nanoparticles as a pH-sensitive system for tumor-targeted delivery of hydrophobic drugs: part 2. In vivo distribution and tumor localization studies. *Pharm. Res.* **22**:2107–2114 (2005).
39. M. S. Chun, S. Y. Lee, and S. M. Yang. Estimation of zeta potential by electrokinetic analysis of ionic fluid flows through a divergent microchannel. *J. Colloid. Interface Sci.* **266**:120–126 (2003).
40. S. Nsereko, and M. Amiji. Localized delivery of paclitaxel in solid tumors from biodegradable chitin microparticle formulations. *Biomaterials*. **23**:2723–2731 (2002).
41. R. T. Liggins, and H. M. Burt. Paclitaxel-loaded poly(L-lactic acid) microspheres 3: blending low and high molecular weight

polymers to control morphology and drug release. *Int. J. Pharm.* **282**:61–71 (2004).
42. M. Zaffaroni, R. Frapolli, T. Colombo, R. Fruscio, E. Bombardelli, P. Morazzoni, A. Riva, M. D'Incalci, and M. Zucchetti. High-performance liquid chromatographic assay for the determination of the novel C-Seco-taxane derivative (IDN 5390) in mouse plasma. *J. Chromatogr. B Analyt. Technol. Biomed. Life Sci.* **780**:93–98 (2002).
43. H. Devalapally, Z. Duan, M. V. Seiden, and M. M. Amiji. Paclitaxel and ceramide co-administration in biodegradable polymeric nanoparticulate delivery system to overcome drug resistance in ovarian cancer. *Int. J. Cancer.* **121**:1830–1838 (2007).